

Published in final edited form as:

Cancer Immunol Res. 2018 November ; 6(11): 1292–1300. doi:10.1158/2326-6066.CIR-18-0038.

Restoration of endogenous retrovirus infectivity impacts mouse cancer models

Eleonora Ottina¹, Prisca Levy¹, Urszula Eksmond¹, Julia Merkschlager¹, George R. Young³, Juliette Roels¹, Jonathan P. Stoye^{3,5}, Thomas Tüting⁴, Dinis P. Calado², and George Kassiotis^{1,5,*}

¹Retroviral Immunology, The Francis Crick Institute, 1 Midland Road, London NW1 1AT, UK

²Immunity & Cancer Laboratory, The Francis Crick Institute, 1 Midland Road, London NW1 1AT, UK

³Retrovirus-Host Interactions, The Francis Crick Institute, 1 Midland Road, London NW1 1AT, UK

⁴Laboratory of Experimental Dermatology, Department of Dermatology, University of Magdeburg, 39120 Magdeburg, Germany

⁵Department of Medicine, Faculty of Medicine, Imperial College London W2 1PG, UK

Abstract

Mouse models have been instrumental in establishing fundamental principles of cancer initiation and progression and continue to be invaluable in the discovery and further development of cancer therapies. Nevertheless, important aspects of human disease are imperfectly approximated in mouse models, notably the involvement of endogenous retroviruses (ERVs). Replication-defective ERVs, present in both humans and mice, may affect tumor development and antitumor immunity through mechanisms not involving infection. Here, we revealed an adverse effect of murine ERVs with restored infectivity on the behavior of mouse cancer models. In contrast to human cancer, where infectious ERVs have never been detected, we found that ERV infectivity was frequently restored in transplantable, as well as genetic, mouse cancer models. Such replication-competent, ERV-derived retroviruses were responsible for unusually high expression of retroviral nucleic acids and proteins in mouse cancers. Infectious ERV-derived retroviruses produced by mouse cancer cells could directly infect tumor-infiltrating host immune cells and fundamentally modified the host's immune defenses to cancer, as well as the outcome of immunotherapy. Therefore, infectious retroviruses, variably arising in mouse cancer models, but not in human cancer, have the potential to confound many immunological studies and should be considered as a variable, if not altogether avoided.

* **Correspondence:** Dr. George Kassiotis, The Francis Crick Institute, 1 Midland Road, London NW1 1AT, UK. T: 44 (0) 20379 61483. george.kassiotis@crick.ac.uk.

Disclosure of Potential Conflicts of Interest

G.K. is a scientific co-founder of and consulting for ERVAXX and a member of its scientific advisory board. None of the other authors have any potential conflicts of interest.

Keywords

Endogenous retroviruses; antitumor immunity; cancer; mouse models; retroviral infectivity

Introduction

Endogenous retroviruses (ERVs), originally discovered as cancer-causing genetic elements (1), can affect multiple aspects of host physiology and pathology, including cancer initiation and progression (2–4). Despite comprising a comparable proportion of the respective genomes, murine and human endogenous retroviruses (ERVs) are phylogenetically distinct (5). Species-specific ERV characteristics should, therefore, be considered in the use of animal models for human diseases, particularly in mouse cancer models.

Murine ERVs are generally, but not exclusively, replication-defective due to accumulation of different mutations in distinct endogenous proviruses or in cellular receptors. For example, laboratory mouse strains produce xenotropic murine leukemia viruses (MLVs) that, although not infectious to murine cells due to mutations in the xenotropic and polytropic retrovirus receptor 1 (Xpr1), are capable of infecting human cell lines propagated in mice (6). The consequences of such infections are exemplified in the emergence of the xenotropic murine leukemia virus-related virus (XMRV), a recombinant contaminant virus in human prostate cancer cells propagated in mice (6). Retroviruses with restored infectivity to murine cells through recombination have been discovered in mouse melanoma and neuroblastoma cell lines and have been implicated in tumor growth (7–9). Restoration of ERV infectivity is also characteristic of immunodeficient mouse colonies on the C57BL/6 (B6) genetic background (10,11), suggesting that such recombination events occur *in vivo* more frequently than previously estimated.

Although ERV expression is upregulated in human cancer and certain human cancer lines produce retroviral particles, no evidence for replication of an ERV-derived retrovirus in humans has yet been reported (12,13). Thus, ERV-derived infectious retroviruses are restricted to mouse models, where diseases may be unwittingly studied in the setting of a retroviral infection. Here, we examined how frequently ERV infectivity is restored in mouse cancers and found an extensive, but not universal presence, of infectious retroviruses in transplantable, as well as genetic mouse cancer models. We found that ERV-derived infectious retroviruses produced by cancer cells can infect tumor-infiltrating immune cells and fundamentally alter disease outcome. Thus, potential production of infectious retroviruses in mouse cancer models is a variable that should be considered in outcome interpretation.

Materials and Methods

Mice

Inbred C57BL/6J (B6), CBA/J, and CD45.1⁺ congenic B6 (B6.SJL-*Ptprca*^a *Pep3*^b/BoyJ) mice were originally obtained from The Jackson Laboratory (Bar Harbor, ME, USA) and subsequently maintained at the Francis Crick Institute's animal facilities. Endogenous

ecotropic MLV-deficient (*Emv2*^{-/-}) mice, additionally rendered CD45.1⁺ or *Rag1*-deficient, were generated in the Kassiotis lab and have been previously described (14). Mice with conditional deletion of *Prdm1* (the gene encoding Blimp1), induced in B cells at early stages of the germinal center reaction by expression of a Cγ1-Cre transgene, have been previously described (15). Mice bearing the conditional allele of *Prdm1* or the Cγ1-Cre transgene were provided by Drs. Alexander Tarakhovsky (The Rockefeller University, New York, USA) and Klaus Rajewsky (Max Delbrück Center for Molecular Medicine, Berlin Germany), respectively (15) and were intercrossed in the Calado lab. Eight to twelve-week old male and female gender-matched recipient mice were used for all experiments. All animal experiments were approved by the ethical committee of the Francis Crick Institute and conducted according to local guidelines and UK Home Office regulations under the Animals Scientific Procedures Act 1986 (ASPA).

Retroviral vectors

Open reading frames encoding either the wild-type (WT) *Emv2* envelope glycoprotein (WT *Emv2env*) or a variant with an E552R and A558F double mutation (E14R and A20F in the ISD; *Emv2envDM*) were synthesized and cloned into the pRV-GFP vector, constructed and kindly provided by Dr. Gitta Stockinger (The Francis Crick Institute, London, UK). Gene synthesis, cloning, and mutagenesis were performed by Genewiz LLC and verified by sequencing. Vesicular stomatitis virus glycoprotein (VSVg)-pseudotyped retroviral particles were produced by transfection, using GeneJuice (EMD Millipore Billerica MA, USA), of 3 μg of either WT *Emv2env* or *Emv2envDM* vector plasmids, together with 3 μg packaging (pHIT60) and 3 μg VSVg-expressing (pcVG-wt) plasmids (both obtained from the Stoye lab) into 3×10⁵ 293T cells. Virus-containing supernatants were collected 48 hours post transfection, passed through a 0.45-μm filter and stored at -80°C until further use.

Cell lines, infections, and transductions

B6-derived B16-F0 cells (CRL-6322), EL4.BU (TIB-40), LL/2 (CRL-1642), CTLL-2 (TIB-21), and JAWSII (CRL-11904) cells were obtained from ATCC. EL4 (TIB-39) cells and chicken ovalbumin-expressing EL4 variant E.G7-OVA (CRL-2113) cells were kindly provided by Drs. Brigitta Stockinger and Caetano Reis e Sousa, respectively, at the Francis Crick Institute, London, UK. HcMel3, HcMel12, HcMel17 and HcMel31 melanoma cells were established independently from primary 7,12-dimethyl-1,2-benzanthracene (DMBA)-induced melanomas in individual HGF-CDK4(R24C) mice (16,17). Melanoma cells expressing the *Braf*^{V600E} form were originally established from mice expressing an inducible *Braf*^{V600E} allele, specifically in melanocytes (18) and were kindly provided by Dr. Richard Marais at the University of Manchester (Manchester, UK) through Dr. Caetano Reis e Sousa at the Francis Crick Institute (London, UK). MCA-38 cells were kindly provided by Dr. Giorgio Trinchieri (National Cancer Institute, Bethesda, MD, USA). MCA-205 cells were kindly provided by Dr. Thomas Blankenstein (Max-Delbrück-Center for Molecular Medicine, Berlin, Germany). DC2.4 cells were kindly provided by Dr. Kenneth Rock (University of Massachusetts Medical School, Worcester MA, USA). 2695 cells were established in the Calado lab, from a diffuse large B cell lymphoma that developed following conditional deletion of *Prdm1* (encoding Blimp1) in class-switching B cells (15) and were passaged once in a WT B6 host. A1 and G7 cells were isolated from progenitor B-cell

lymphomas that developed in IL7-overexpressing mice, as previously described (19), and were kindly provided by Dr. Amanda Fisher.

Cells were grown in Iscove's Modified Dulbecco's Medium (IMDM) (Sigma-Aldrich, St. Louis, MO, USA) supplemented with 5%-10% fetal bovine serum (Gibco, Thermo Fisher Scientific, Waltham, MA USA), 2 mM L-glutamine, penicillin (100 U/mL) and streptomycin (0.1 mg/mL). JAWSII cells were grown in the same medium additionally supplemented with recombinant GM-CSF (20 ng/mL; Peprotech Ltd, Rocky Hill, NJ, USA). HCmel cell lines were grown in Minimum Essential Media (MEM) supplemented with non-essential amino acids (Gibco). All cell lines (Supplementary Table S1) were verified as murine and were mycoplasma free. Species identification was carried out by the Cell Services facility at the Francis Crick Institute, using previously established multiplex PCR assays (20,21). Transplantable cancer cell lines were passaged for a maximum 18-24 times or kept for a maximum of 8 weeks in culture.

MCA-38 and MCA-205 cells producing GFP-encoding transducing retroviral particles were generated by transduction of the replication-defective XG7 retroviral vector, which encompasses a neomycin resistance gene (*neo*) under the control of the long terminal repeat (LTR) and a GFP-encoding gene driven by the human cytomegalovirus (CMV) promoter, as previously described (10). *Mus dunni* fibroblast cells (*M. dunni* cells; CRL-2017), kindly provided by the Stoye lab, were used for the viral infectivity assays as previously described (10). Infections and transductions were carried out by adding serial dilutions of the viral stocks to target cells in the presence of polybrene (4 µg/mL). EL4 sublines transduced with WT *Emv2env* or *Emv2envDM* were established by cell sorting, based on GFP and envelope expression, performed on a FACS ARIA Fusion (BD Biosciences).

Sequencing

Part of the *pol* open reading frame of was sequenced from virion genomes as previously described (10). Briefly, RNA was extracted from culture supernatant of the EL4.BU, MCA-205 MCA-38 and HCmel12 tumor cell lines using the QIAamp viral RNA mini Kit (Qiagen, Hilden, Germany) and then reverse-transcribed using SuperScript IV Reverse Transcriptase (Thermo Fisher). The first half of retroviral genomes was amplified using Ranger DNA polymerase (Bioline) and the following primers: Forward 5'-GCGCCAGTCTCCGATAGACT-3'; Reverse 5'-CCGGGAGAGGGAGTAAGGTGGC-3'. Amplicons were purified with the QIAquick PCR purification kit (Qiagen) and then subjected to Sanger sequencing at the Francis Crick Institute using the same primers. Sequence analyses, comparisons, and alignments were performed with Vector NTI v11.5 (Invitrogen).

Tumor challenge and immunotherapy

Tumor challenge was initiated by subcutaneous inoculation of tumor cell suspensions into the right flank of recipient mice. One million XG7-transduced MCA-38 or MCA-205 cells were inoculated into (CBA×B6) F₁ hosts, which were monitored three times per week for up to 21 days. Two million EL4 or EL4.BU cells were inoculated into CD45.2⁺ or CD45.1⁺ congenic B6 or *Emv2*^{-/-} hosts, which were monitored three times per week for up to 11

days. Tumor sizes (cm²) were determined by caliper measurements of two axes and calculated using the formula: $\pi \times a \times b$, where a = half of length and b = half of width of the tumors. These measurements taken from live animals were confirmed by additional caliper measurements and weighing of the resected tumor mass at the end of the observation period. For the immunotherapy studies, mice received intraperitoneal injections of 200 μ g anti-PD-L1 (clone 10F.9G2; BioXCell, West Lebanon, NH, USA) and 100 μ g anti-CTLA-4 (clone UC10-4F10-11; BioXCell) on days 1, 4, and 7 post tumor inoculation.

Flow cytometry and cell sorting

Single-cell suspensions were prepared from freshly isolated tumors and lymph nodes, using mechanical and enzymatic digestion. Briefly, tumors and draining lymph nodes were resected and diced in 2 mL of IMDM medium supplemented with Liberase TL (100 μ g/mL; Roche, Mannheim, Germany) and DNaseI (50 μ g/mL; Roche). Digests were performed at 37°C, with periodic vortexing. The enzymatic activity was stopped with the addition of 5 mL IMDM supplemented with 5% FCS to each sample. The samples were then mechanically disrupted, using syringe plungers and strained through a nylon filter with a pore size of 70 μ m (Fisher) to obtain a single-cell suspension. Flow cytometry analysis was performed with the following monoclonal antibodies: 53-6.7 anti-CD8; M1/70 anti-CD11b; IM7 anti-CD44; A20 anti-CD45.1; 104 anti-CD45.2 purchased from BioLegend (San Diego, CA, USA); and RA3-6B2 anti-B220; GK1.5 anti-CD4; N418 anti-CD11c; RB6-8C5 anti-Gr-1; M5/114.152 anti-MHCII; H57-597 anti-TCR β purchased from eBioscience (San Diego, CA, USA). Samples were stained with antibody mixtures for 20 minutes at room temperature and analyzed on an LSR Fortessa X20 cell analyzer.

Tumor cell and host T-cell sorting was performed using anti-CD4-eFlour450 (clone RM4-5, eBioscience), anti-CD8-FITC (clone 53-6.7, eBioscience), anti-CD45.1-PE-Cy7 (clone A20, Biolegend), anti-CD45.2-APC (clone 104, eBioscience), anti-TCRb-APCeFluor780 (clone H57-597, eBioscience) on a BD FACS Aria Fusion (BD Biosciences) or MoFlo XDP (Beckman Coulter, Brea, CA, USA) cell sorters. Purity was checked by flow cytometry analysis of the sorted cells on the BD FACS Aria Fusion or MoFlo XDP and was more than 95%.

MLV detection and quantitation

MLV envelope glycoprotein expression in cell lines was detected by flow cytometry using the 83A25 monoclonal antibody, as previously described (10). MLV RNA expression in cancer cells was determined by real-time quantitative reverse transcription-based PCR (qRT-PCR), starting with cell-associated RNA isolated from 10⁶ tumor cells collected in RLT buffer (Qiagen). RNA was extracted using RNeasy Mini QIAcube Kit (Quiagen) and treated with 0.15 Kunitz units DNaseI (Quiagen). cDNA was produced using High-Capacity Reverse Transcription kit (Applied Biosystems - Thermo Fisher) with RNasin ribonuclease inhibitor (Promega, Madison, WI, USA). The amplification products were then purified using the QIAquick PCR purification kit (Qiagen) and eluted in 30 μ L RNase-free water (Qiagen). 1 μ L eluted cDNA was then used as template for quantitative PCR using Fast SYBR Green (Applied Biosystems), using primers listed in Supplementary Table S2, as previously described (10). Data are plotted as expression of the target transcript, relative to

expression of *Hprt* in the same sample using the 2^{-Ct} method. Quantification of MLV virion-associated RNA produced by tumor cell lines was determined by qRT-PCR on RNA extracted from 140 μ L cell culture supernatant using the QIAamp viral RNA mini Kit (Qiagen) with carrier RNA (8 μ g/mL) according to the manufacturer's protocol. B6 genomic DNA, which carries a defined number of copies of each MLV group, was used as a standard to allow quantitation of MLV genome copies in tumor cell culture supernatants.

Mitigation of *in vitro* MLV infection

To exclude the possibility of inadvertent infection of tumor cell lines during their life history in our or other labs, the following steps were taken. Firstly, samples were obtained for testing directly from the donating labs (2695 and Braf^{V600E}) or were confirmed positive by testing at the donating labs (MCA-38). Secondly, elevated eMLV expression was also confirmed by RNA-sequencing of spontaneous B-cell lymphomas from individual mice with deregulated BCL6 and NF- κ B expression restricted to the germinal center lineage B cells (22) before any *ex vivo* or *in vitro* culture or other manipulation. Thirdly, HcMel31 melanoma cells that remained virus-free throughout our studies at both the donating and receiving labs were readily infected if deliberately exposed to virus produced by HcMel12 cells, arguing against inadvertent spread of infectious MLVs *in vitro*.

Assessment of MLV infection

To determine the *in vitro* infectivity of MLV virions produced by tumor cells, 1:2 to 1:30 serial dilutions of tumor cell culture supernatants were added to permissive *Mus dunni* fibroblast cells, plated in 96 well-plates at 2×10^4 cells/mL (100 μ L per well) in the presence of polybrene (4 μ g/mL). MLV infection of target *Mus dunni* cells was detected three days later by flow cytometry, using the 83A25 antibody.

MLV infection of host cells *in vivo* was assessed first by acquisition of GFP expression in host cells identified by flow cytometry and, secondly, by qPCR detection of vector-contained *neo* sequences in genomic DNA from purified tumor-infiltrating TCR β^+ T cells. MLV infection of *Emv2^{-/-}* host TCR β^+ T cells infiltrating EL4 and EL4.BU tumors was assessed by qPCR for the eMLV *env* gene, which is absent from these hosts (14). Briefly, sorted cells were collected in 500 μ L lysis buffer (100 mM Tris-HCl pH8.5, 5 mM EDTA, 200 mM NaCl, 0.2% SDS) and digested by Proteinase K (0.2 mg/mL; Sigma-Aldrich) for 2 hours at 56°C. Released DNA was then purified by ethanol precipitation and used as template for PCR amplification at ~600 ng/reaction in duplicate reactions. In both cases, DNA copies of *neo* and eMLV *env* genes in host TCR β^+ T cells were normalized according to the single copy *Ifnar1* gene using a 2^{-Ct} method, as previously described (10) (Supplementary Table S2).

Expression analysis of tumor-infiltrating T cells

CD4⁺ and CD8⁺ T cells (CD45.1⁺TCR β^+) were purified from tumor cell suspensions by sorting (described above) and total RNA was extracted using the RNeasy Mini QIAcube Kit (Qiagen). Transcription of key effector molecules was assessed by qRT-PCR, as described in the previous section for MLV detection and quantitation, using primers listed in Supplementary Table S2.

Statistical analysis

Statistical comparisons were made using SigmaPlot 13.0 (Systat Software Inc., Germany). Parametric comparisons of normally-distributed values that satisfied the variance criteria were made by unpaired Student's t-tests or one-way Analysis of variance (ANOVA) tests. Data that did not pass the variance test were compared with non-parametric, two-tailed Mann-Whitney Rank Sum tests or ANOVA on Ranks tests. *P* values less than 0.05 were considered significant. Heat-maps were produced using the Qlucore Omics Explorer (Qlucore, Lund, Sweden).

Results and Discussion

B6 mice are the most commonly used mouse strain, naturally lacking endogenous MLVs able to replicate in mouse cells. Nevertheless, infectious ecotropic MLVs can emerge through recombination between defective ERVs in cancer cell lines (23). Although replication-defective germline MLVs do express low levels of retroviral proteins, *de novo* and often multiple infection of cancer cell lines by infectious MLVs leads to elevated expression of retroviral proteins. To examine how common infectious MLVs are in B6-derived tumors, we screened a panel of cell lines for elevated MLV envelope glycoprotein expression. In addition to B16 melanoma cells, high expression of MLV envelope was detected in *Braf*^{V600E} melanoma cells (Fig. 1A), originally derived from mice expressing an inducible *Braf*^{V600E} allele in melanocytes (18). High MLV envelope expression was detected in 3 out of 4 melanoma transplant lines (HCmel3, HCmel12, HCmel17, and HCmel31) (Fig. 1A), which were chemically induced in melanoma-prone transgenic mice overexpressing hepatocyte growth factor (HGF) and an oncogenic CDK4(R24C) mutation (16,17). High expression of MLV envelope was also observed in chemically-induced MCA-38 colon adenocarcinoma and MCA-205 fibrosarcoma cells, as well as in spontaneous LL/2 Lewis lung carcinoma cells (Fig. 1A). In contrast to the parental chemically-induced T-cell lymphoma EL4 cell line, high MLV envelope expression was seen in the BrdU-resistant EL4.BU and the chicken ovalbumin-expressing E.G7-OVA sublines of EL4 cells (Fig. 1A). Intermediate MLV envelope expression was observed in the immature dendritic cell line JAWSII, established from a *Trp53*^{-/-} mouse and the oncogene-transformed DC2.4 dendritic cell line (24), whereas the IL2-dependent CTLL-2 T-cell line was negative (Fig. 1A). High MLV envelope expression could also be detected in certain primary tumors from genetic cancer models. A diffuse large B cell lymphoma, termed 2695, from mice with conditional deletion of *Prdm1* (encoding Blimp1) in early germinal center B cells (15), was positive for MLV envelope expression (Fig. 1A). Two progenitor B cell lymphomas, A1 and G7, from IL7-overexpressing mice (19), also expressed MLV envelope, albeit intermediately (Fig. 1A).

We next used PCR-based methods to distinguish between the four host-tropism types of MLV, which could be responsible for MLV envelope expression. B16, *Braf*^{V600E}, HCmel3, HCmel12, HCmel17, MCA-38, MCA-205, LL/2, EL4.BU, and E.G7-OVA cells had high expression of ecotropic MLV (eMLV), but not of polytropic, modified polytropic, or xenotropic MLV (pMLV, mpMLV, and xMLV, respectively) *env* RNA (Fig. 1B). All 8 of these cell lines also produced high amounts of virions containing eMLV *env* RNA, and

MCA-205 and LL/2 additionally produced pMLV *env* RNA-containing virions (Fig. 1B). In contrast, HCmel31, EL4, JAWSII, DC2.4, and CTLL-2 cells expressed only low cell-associated eMLV *env* RNA (Fig. 1B), transcribed from the germline *Emv2* copy in B6 cells (14), and they did not produce eMLV *env* RNA-containing virions (Fig. 1B). Thus, established and primary tumor cell lines displayed variable induction of endogenous MLV expression, and many produced potentially infectious eMLV virions. All cell lines exhibiting high expression of eMLV also produced virions that caused direct infection of target *Mus dunnii* cells *in vitro* (Supplementary Fig. S1), with the possible exception of LL/2 cells.

Similarly to the recombinant MLV, termed MelARV, first described in B16 melanoma cells (25), it was likely that infectious MLVs present in other tumor cell lines were also *de novo* generated. To examine this and exclude the possibility of inadvertent contamination, we took a number of steps (please see Materials and Methods: Mitigation of *in vitro* MLV infection), including deliberate infection of the virus-free HCmel31 cell line (Supplementary Fig. S2), which served as sentinel for any *in vitro* spreading viruses. In addition to these steps, sequencing of the region of the *pol* open reading frame, that carries the reverse transcriptase-inactivating mutation in *Emv2*, revealed the presence of related, but distinct, viruses in the supernatant of EL4.BU, MCA-38, MCA-205, and HCmel12 cells (Supplementary Fig. S3), again supporting *de novo* restoration of infectivity.

Mouse cancer models most typically involve inoculation of tumor cells, potentially producing infectious eMLVs, which could, in principle, infect host cells. To detect and estimate the frequency of such events, we introduced a replication-defective retroviral vector expressing GFP into MCA-38 and MCA-205 cells prior to inoculation. Replication-competent MLV virions produced by such cells would also encapsidate this vector, marking infected host cells with GFP expression (10). In contrast to immune cell types in the lymph nodes draining the subcutaneous site of MCA-38 cell inoculation, those infiltrating the retrovirally transduced tumors comprised significant proportions (between 10% and 50%) of GFP-positive cells (Fig. 2A-C), indicating direct infection by pseudo-typed GFP-encoding vectors. Comparable results were also obtained when MCA-205 cells were similarly used (Fig. 2C). GFP expression in tumor-infiltrating lymphocytes (TILs) was accompanied by the presence of neomycin-encoding DNA, which is also included in the transducing retroviral vector, detected by PCR (Fig. 2D). Thus, tumor cell inoculation into recipient mice resulted in infection of a considerable proportion of host immune cells infiltrating the tumor mass, but not to systemic infection of the host, consistent with limited spread of ERV-derived infectious MLVs in immunocompetent mice (10).

To examine the impact of infectious MLV production during a typical *in vivo* tumor challenge experiment, we compared the infectious virus-positive EL4.BU subline with the parental EL4 line. Immunity against EL4 cells *in vivo* was examined in two different experimental systems: firstly, by using hosts that were naturally reactive against eMLV antigens, and secondly, by checkpoint blockade in WT hosts. For the former, we employed mice deficient in *Emv2*, the single-copy defective eMLV provirus in B6 mice (14). Lack of germline eMLV sequences in *Emv2*^{-/-} mice permitted detection of host cell somatic infection by tumor cell-produced eMLV. *Emv2*^{-/-} host T cells isolated from subcutaneous

EL4.BU, but not EL4 tumors, acquired eMLV *env* DNA, supporting *in vivo* infectivity of EL4.BU-produced eMLV virions (Supplementary Fig. S4A).

Lack of immunological tolerance to eMLV products in *Emv2*^{-/-} mice leads to strong immune reactivity against eMLV (14). Products of eMLVs from the defective germline *Emv2* provirus had low expression in EL4 cells and higher expression additionally from *de novo* eMLV re-infection in EL4.BU cells (Supplementary Fig. S4B). In both cases, eMLV products served as tumor-specific antigens, which are recognized by the *Emv2*^{-/-} hosts.

EL4 and EL4.BU tumors grew comparably in partially eMLV-tolerant WT B6 hosts (Fig. 3A-C) and in virus-free immunodeficient *Rag1*^{-/-}*Emv2*^{-/-} hosts (Supplementary Fig. S4C), arguing against intrinsic growth differences between the two sublines. As predicted by their stronger immune responses targeting the low expression of *Emv2* in EL4 cells, *Emv2*^{-/-} hosts exhibited significant resistance to EL4 tumor growth (Fig. 3A-C). However, immune-mediated resistance of *Emv2*^{-/-} hosts was lost when EL4.BU cells were used, which grew similarly regardless of host immune status (Fig. 3A-C). Thus, the presence of infectious eMLVs in EL4.BU cells appeared to overcome antitumor immunity.

Immune-mediated rejection of EL4 cells in *Emv2*^{-/-} hosts was accompanied by host immune cell infiltration and, in most cases, outnumbering tumor cells (Supplementary Fig. S5 and Fig. 3D). In contrast, immune cell infiltration of EL4.BU tumors was comparably low in both *Emv2*^{-/-} and WT hosts (Supplementary Fig. S5 and Fig. 3D). Enhanced immune reactivity of *Emv2*^{-/-} hosts was also reflected in altered immune infiltrate composition (Fig. 3E). The proportional increase in myeloid cell and CD8⁺ T-cell infiltrates that characterized the stronger response of *Emv2*^{-/-} hosts to EL4 tumors was also present when *Emv2*^{-/-}, but not WT, hosts were inoculated with EL4.BU tumors (Fig. 3E), suggesting that an immune response to EL4.BU cells was initiated in *Emv2*^{-/-} hosts but not propagated. Support of a quantitative, rather than qualitative, effect of infectious eMLVs in EL4.BU cells on the antitumor immune response was also provided by transcription of key effector molecules in TILs (Fig. 3F).

Similarly to the natural antitumor immunity in *Emv2*^{-/-} hosts, antitumor immunity boosted by checkpoint blockade in partially eMLV-tolerant WT hosts was disparately effective against EL4 and EL4.BU tumor challenge. Treatment of WT hosts with anti-CTLA-4 and anti-PD-L1 led to near complete growth control of EL4 tumors (Fig. 4A-C). In contrast, the same treatment was largely ineffective against EL4.BU tumors (Fig. 4A-C). Accordingly, anti-CTLA-4 and anti-PD-L1 treatment significantly increased the overall numbers of tumor-infiltrating host immune cells in EL4, but not EL4.BU tumors (Fig. 4D). Together, these results suggest that the presence of infectious virus in the EL4.BU subline substantially reduces its responsiveness to immunotherapy.

Although not yet fully appreciated, the impact of infectious eMLV in the course of EL4.BU tumor challenge includes, at a minimum, severe numerical reduction of local antitumor immunity. Some retroviral envelope glycoproteins are considered inherently immunosuppressive, a property mapped to a defined domain of a conserved domain, termed the immunosuppressive domain (ISD), in the transmembrane (TM) subunit (26–28).

Consequently, the immune suppressive effects of EL4.BU tumors could arise from the elevated expression of MLV envelope glycoprotein in these cells. It should be noted, however, that this elevated MLV envelope expression in EL4.BU cells resulted from re-infection of these cells with eMLVs because the expression of *de novo* acquired proviruses is higher than that of the germline counterparts (10).

Nevertheless, to examine a possible contribution of the ISD to the reduction of antitumor immunity, we transduced infectious virus-free EL4 cells with retroviral vectors encoding either the WT *Emv2* envelope glycoprotein (EL4.*Emv2env*) or a variant of bearing mutations in two key residues (E14R and A20F in the ISD) (Supplementary Fig. S6A-D), previously thought to affect immunosuppressive activity (EL4.*Emv2envDM*) (28). In comparison with the parental EL4 cells, overexpression of either form of *Emv2* envelope slightly reduced the growth of transduced EL4 cells in WT B6 hosts (Fig. 4E-G). However, the growth of EL4.*Emv2env* and EL4.*Emv2envDM* cells was not significantly different (Fig. 4E-G). Similarly, both EL4.*Emv2env* and EL4.*Emv2envDM* cells were rejected in *Emv2*^{-/-} hosts as efficiently as the parental EL4 cells (Fig. 4E-G). Thus, the unaffected rejection of *Emv2* envelope-overexpressing EL4 cells in *Emv2*^{-/-} hosts and slower growth in WT B6 hosts, regardless of the presence or absence of the ISD double mutation, argue against a dominant contribution of the immunosuppressive activity of the envelope glycoprotein, outside the context of viral infection. Our recent work has indicated that the previously described double mutation in the ISD compromises virus infectivity (29). Therefore, a more parsimonious explanation for the immunosuppressive effect of infectious MLV-producing EL4.BU cells is direct infection of host immune cells. Such infection would alter the physiology of host immune cells, as well as render them targets for anti-MLV host immune responses.

Regardless of its precise mechanism, the attenuation of antitumor adaptive immunity by tumor-produced infectious MLVs modifies fundamental tumor model properties, such as natural responses to a tumor-associated antigen or response to immunotherapy. Innate immune recognition of tumor cells, currently considered to involve ERV nucleic acids (30,31), will also be inevitably affected by infectious retroviral particles in certain mouse cancer models. Replication-defective ERVs may well play a critical role in antitumor immunity in humans (32) and warrant further investigation. The use of mouse models, however, to extrapolate the involvement of human ERVs in cancer should not be complicated by the accidental presence of infectious retroviruses. Based on these findings, we propose that the presence of infectious MLVs in mouse cancer models should be considered as biological contamination. As such, it should be documented, if not entirely prevented in mouse cancer studies to prevent misinterpretation of the results or mistranslation to human cancer.

Supplementary Material

Refer to Web version on PubMed Central for supplementary material.

Acknowledgments

We wish to thank Drs. Giorgio Trinchieri for the MCA-38 cells and for instrumental discussion, Thomas Blankenstein for the MCA-205 cells, Kenneth Rock for the DC2.4 cells, Richard Marias for the Braf^{V600E} cells and Amanda Fisher for the A1 and G7 cells. We are grateful for assistance from the Biological Research and Flow Cytometry Facilities at the Francis Crick Institute.

Funding: This work was supported by the Francis Crick Institute (FC001099 to G.K., FC001162 to J.P.S., FC001057 to D.P.C.), which receives its core funding from Cancer Research UK the UK Medical Research Council and the Wellcome Trust; and by the Wellcome Trust (102898/B/13/Z to G.K.).

References

1. Weiss RA. The discovery of endogenous retroviruses. *Retrovirology*. 2006; 3:67. [PubMed: 17018135]
2. Kassiotis G. Endogenous retroviruses and the development of cancer. *J Immunol*. 2014; 192(4): 1343–9. [PubMed: 24511094]
3. Cherkasova E, Weisman Q, Childs RW. Endogenous retroviruses as targets for antitumor immunity in renal cell cancer and other tumors. *Front Oncol*. 2013; 3:243. [PubMed: 24062992]
4. Downey RF, Sullivan FJ, Wang-Johanning F, Ambs S, Giles FJ, Glynn SA. Human endogenous retrovirus K and cancer: Innocent bystander or tumorigenic accomplice? *Int J Cancer*. 2015; 137(6): 1249–57. [PubMed: 24890612]
5. Mager DL, Stoye JP. Mammalian Endogenous Retroviruses. *Microbiol Spectr*. 2015; 3(1)
6. Delviks-Frankenberry K, Cingoz O, Coffin JM, Pathak VK. Recombinant origin, contamination, and de-discovery of XMRV. *Curr Opin Virol*. 2012; 2(4):499–507. [PubMed: 22818188]
7. Li M, Huang X, Zhu Z, Gorelik E. Sequence and Insertion Sites of Murine Melanoma-Associated Retrovirus. *J Virol*. 1999; 73(11):9178–86. [PubMed: 10516025]
8. Pothlichet J, Heidmann T, Mangeney M. A recombinant endogenous retrovirus amplified in a mouse neuroblastoma is involved in tumor growth in vivo. *Int J Cancer*. 2006; 119(4):815–22. [PubMed: 16550601]
9. Pothlichet J, Mangeney M, Heidmann T. Mobility and integration sites of a murine C57BL/6 melanoma endogenous retrovirus involved in tumor progression in vivo. *International journal of cancer*. 2006; 119(8):1869–77. DOI: 10.1002/ijc.22066 [PubMed: 16708391]
10. Young GR, Eksmond U, Salcedo R, Alexopoulou L, Stoye JP, Kassiotis G. Resurrection of endogenous retroviruses in antibody-deficient mice. *Nature*. 2012; 491(7426):774–8. [PubMed: 23103862]
11. Yu P, Lubben W, Slomka H, Gebler J, Konert M, Cai C, et al. Nucleic acid-sensing Toll-like receptors are essential for the control of endogenous retrovirus viremia and ERV-induced tumors. *Immunity*. 2012; 37(5):867–79. [PubMed: 23142781]
12. Voisset C, Weiss RA, Griffiths DJ. Human RNA "rumor" viruses: the search for novel human retroviruses in chronic disease. *Microbiol Mol Biol Rev*. 2008; 72(1):157–96. [PubMed: 18322038]
13. Young GR, Stoye JP, Kassiotis G. Are human endogenous retroviruses pathogenic? An approach to testing the hypothesis. *Bioessays*. 2013; 35(9):794–803. [PubMed: 23864388]
14. Young GR, Ploquin MJ, Eksmond U, Wadwa M, Stoye JP, Kassiotis G. Negative selection by an endogenous retrovirus promotes a higher-avidity CD4+ T cell response to retroviral infection. *PLoS Pathog*. 2012; 8(5):e1002709. [PubMed: 22589728]
15. Calado DP, Zhang B, Srinivasan L, Sasaki Y, Seagal J, Unitt C, et al. Constitutive canonical NF-kappaB activation cooperates with disruption of BLIMP1 in the pathogenesis of activated B cell-like diffuse large cell lymphoma. *Cancer Cell*. 2010; 18(6):580–9. DOI: 10.1016/j.ccr.2010.11.024 [PubMed: 21156282]
16. Bald T, Quast T, Landsberg J, Rogava M, Glodde N, Lopez-Ramos D, et al. Ultraviolet-radiation-induced inflammation promotes angiotropism and metastasis in melanoma. *Nature*. 2014; 507(7490):109–13. DOI: 10.1038/nature13111 [PubMed: 24572365]

17. Landsberg J, Kohlmeyer J, Renn M, Bald T, Rogava M, Cron M, et al. Melanomas resist T-cell therapy through inflammation-induced reversible dedifferentiation. *Nature*. 2012; 490(7420):412–6. DOI: 10.1038/nature11538 [PubMed: 23051752]
18. Dhomen N, Reis-Filho JS, da Rocha Dias S, Hayward R, Savage K, Delmas V, et al. Oncogenic Braf induces melanocyte senescence and melanoma in mice. *Cancer Cell*. 2009; 15(4):294–303. DOI: 10.1016/j.ccr.2009.02.022 [PubMed: 19345328]
19. Fisher AG, Burdet C, LeMeur M, Haasner D, Gerber P, Ceredig R. Lymphoproliferative disorders in an IL-7 transgenic mouse line. *Leukemia*. 1993; 7(Suppl 2):S66–8. [PubMed: 8361236]
20. Cooper JK, Sykes G, King S, Cottrill K, Ivanova NV, Hanner R, et al. Species identification in cell culture: a two-pronged molecular approach. *In vitro cellular & developmental biology Animal*. 2007; 43(10):344–51. DOI: 10.1007/s11626-007-9060-2 [PubMed: 17934781]
21. Ono K, Satoh M, Yoshida T, Ozawa Y, Kohara A, Takeuchi M, et al. Species identification of animal cells by nested PCR targeted to mitochondrial DNA. *In vitro cellular & developmental biology Animal*. 2007; 43(5-6):168–75. DOI: 10.1007/s11626-007-9033-5 [PubMed: 17516125]
22. Attig J, Young GR, Stoye JP, Kassiotis G. Physiological and Pathological Transcriptional Activation of Endogenous Retroelements Assessed by RNA-Sequencing of B Lymphocytes. *Frontiers in microbiology*. 2017; 8:2489.doi: 10.3389/fmicb.2017.02489 [PubMed: 29312197]
23. Leong SP, Muller J, Yetter RA, Gorelik E, Takami T, Hearing VJ. Expression and modulation of a retrovirus-associated antigen by murine melanoma cells. *Cancer Res*. 1988; 48(17):4954–8. [PubMed: 2842042]
24. Shen Z, Reznikoff G, Dranoff G, Rock KL. Cloned dendritic cells can present exogenous antigens on both MHC class I and class II molecules. *J Immunol*. 1997; 158(6):2723–30. [PubMed: 9058806]
25. Li M, Xu F, Muller J, Hearing VJ, Gorelik E. Ecotropic C-type retrovirus of B16 melanoma and malignant transformation of normal melanocytes. *International journal of cancer*. 1998; 76(3):430–6. [PubMed: 9579583]
26. Dupressoir A, Lavialle C, Heidmann T. From ancestral infectious retroviruses to bona fide cellular genes: role of the captured syncytins in placentation. *Placenta*. 2012; 33(9):663–71. [PubMed: 22695103]
27. Kudo-Saito C, Yura M, Yamamoto R, Kawakami Y. Induction of immunoregulatory CD271+ cells by metastatic tumor cells that express human endogenous retrovirus H. *Cancer Res*. 2014; 74(5):1361–70. [PubMed: 24590808]
28. Schlecht-Louf G, Renard M, Mangeney M, Letzelter C, Richaud A, Ducos B, et al. Retroviral infection in vivo requires an immune escape virulence factor encrypted in the envelope protein of oncoretroviruses. *Proc Natl Acad Sci U S A*. 2010; 107(8):3782–7. [PubMed: 20142478]
29. Eksmond U, Jenkins B, Merckenschlager J, Mothes W, Stoye JP, Kassiotis G. Mutation of the Putative Immunosuppressive Domain of the Retroviral Envelope Glycoprotein Compromises Infectivity. *Journal of virology*. 2017; 91(21)doi: 10.1128/jvi.01152-17
30. Bannert N, Hofmann H, Block A, Hohn O. HERVs New Role in Cancer: From Accused Perpetrators to Cheerful Protectors. *Frontiers in microbiology*. 2018; 9:178.doi: 10.3389/fmicb.2018.00178 [PubMed: 29487579]
31. Kassiotis G, Stoye JP. Immune responses to endogenous retroelements: taking the bad with the good. *Nat Rev Immunol*. 2016; 16(4):207–19. DOI: 10.1038/nri.2016.27 [PubMed: 27026073]
32. Kassiotis G, Stoye JP. Making a virtue of necessity: the pleiotropic role of human endogenous retroviruses in cancer. *Philosophical transactions of the Royal Society of London Series B, Biological sciences*. 2017; 372(1732)doi: 10.1098/rstb.2016.0277

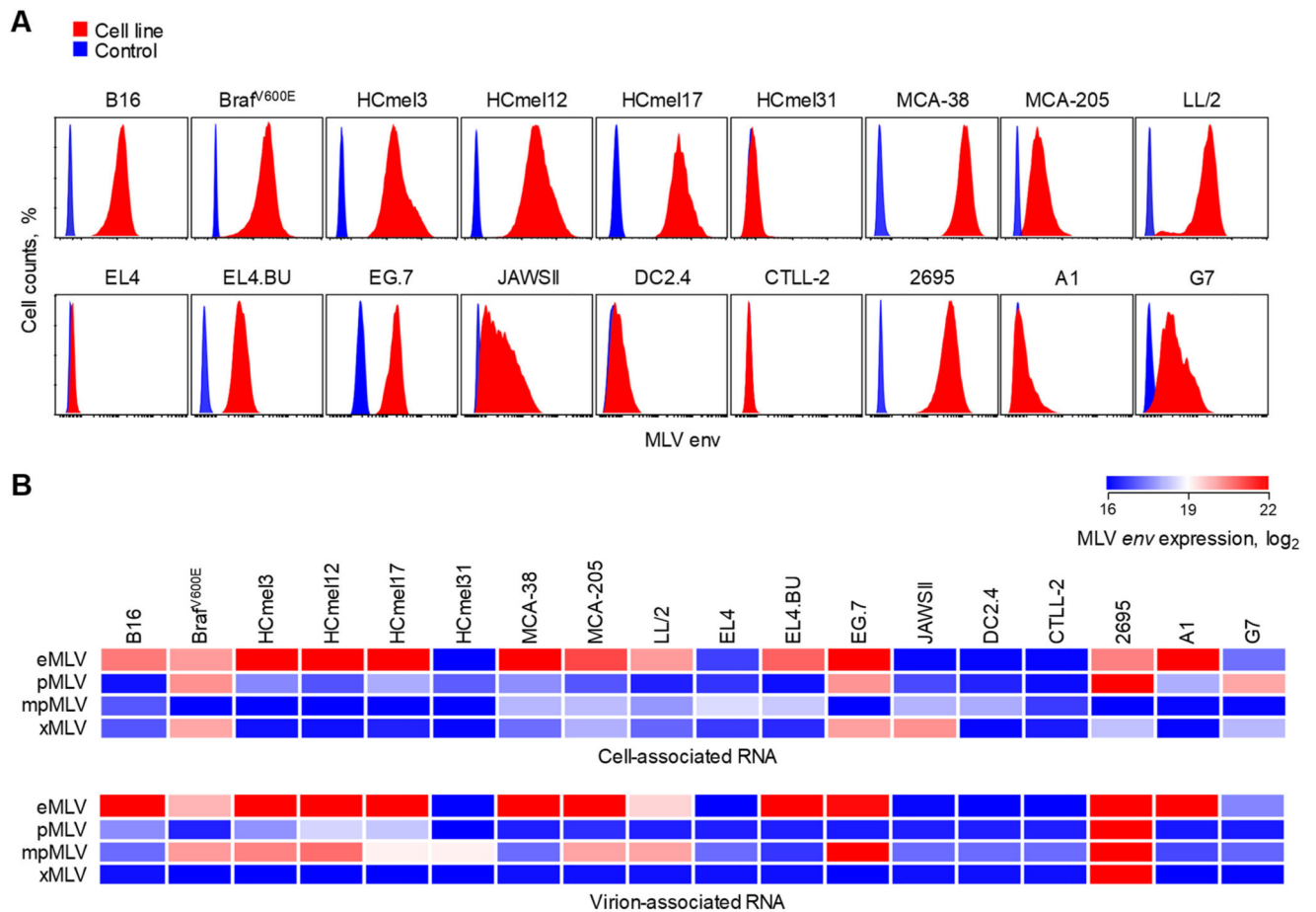


Figure 1. MLV expression in B6-derived cancer cell lines.

A, MLV envelope glycoprotein expression in the indicated cells (red), detected with the 83A25 monoclonal antibody. Controls (blue) represent the staining with the secondary and tertiary reagents only. B, Relative expression of *env* RNA, corresponding to each MLV group and normalized against *Hprt* RNA, in cellular RNA from the indicated cells (cell-associated RNA, *top*) or the presence of *env* RNA per volume unit, corresponding to each MLV group, in the supernatant of the same cells (virion-associated RNA, *bottom*).

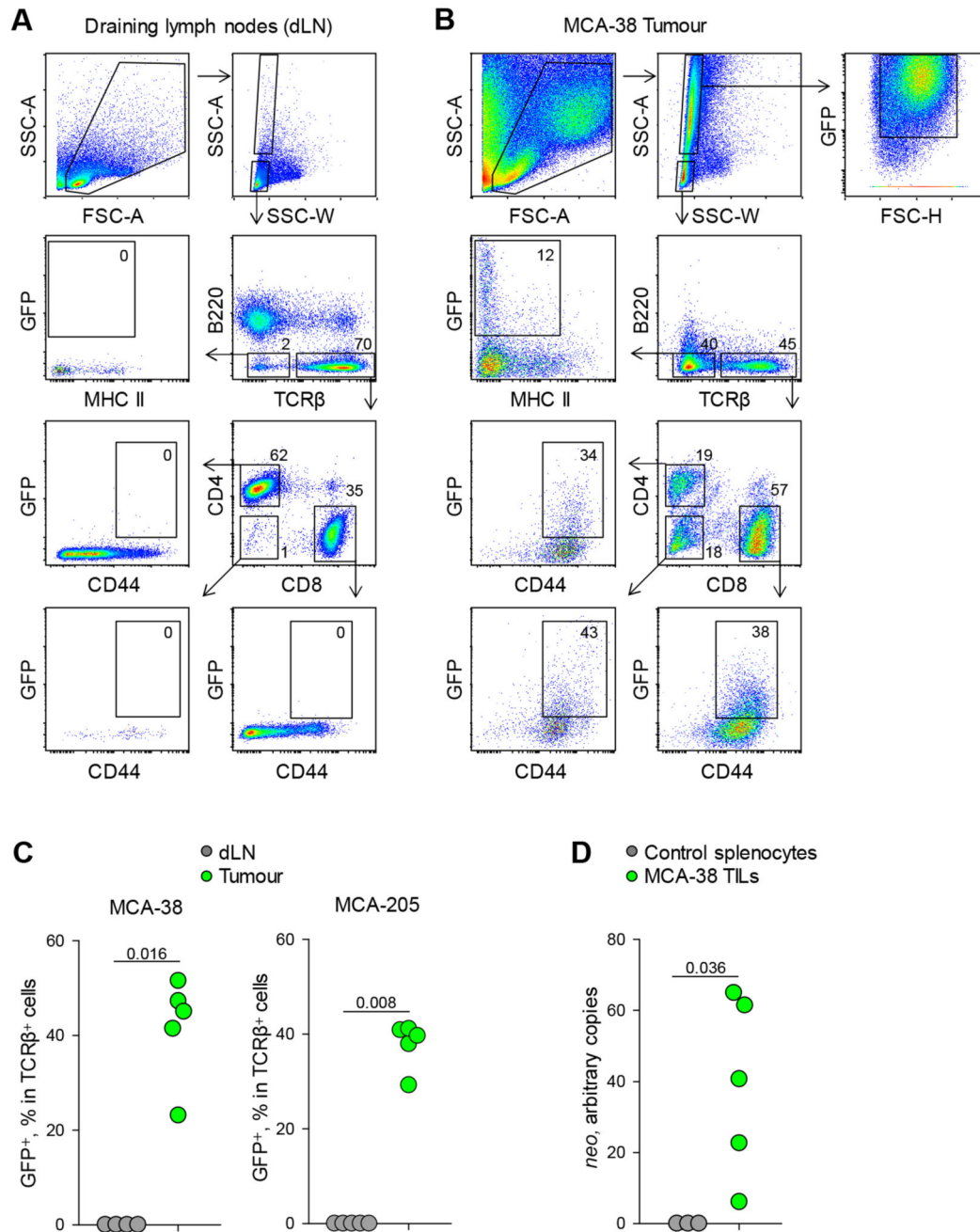


Figure 2. *In vivo* infectivity of MCA-38- and MCA-205-produced MLVs.

A, Retroviral vector-encoded GFP expression in B cells (B220⁺), memory-phenotype (CD44⁺ CD4⁺ or CD8⁺ T cells (TCRβ⁺), or non-lymphocytes (B220⁻ TCRβ⁻) isolated from the tumor-draining (inguinal) lymph nodes (dLNs) of 10 (B6×CBA) F₁ hosts subcutaneously inoculated with 10⁶ MCA-38 cells, which had been transduced with a GFP-encoding retroviral vector. B, GFP expression in cells isolated from the subcutaneous MCA-38 tumor mass of the same mice as in A. C, Frequency of GFP⁺ cells in T cells isolated from dLNs or the subcutaneous tumor mass of MCA-38 (*left*) or MCA-205 (*right*) inoculation. D,

Detection of retroviral vector *neo* DNA in MCA-38 TILs in comparison with lymphocytes from naïve animals. In C and D, each symbol is an individual mouse from one of two independent experiments (5 mice/tumor model). N=10 mice/tumor model were used in two experiments. Numbers within C and D denote the *p* values of two-tailed Mann-Whitney Rank Sum tests.

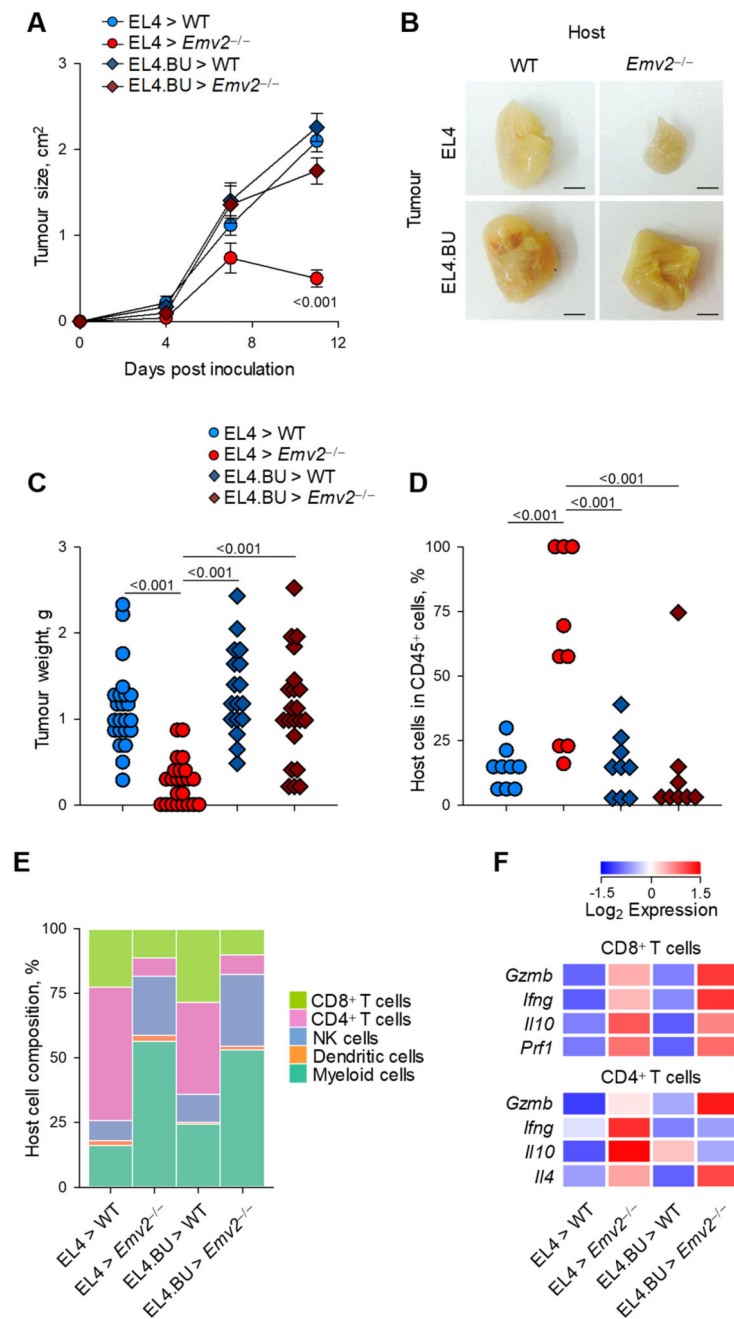


Figure 3. Impact of infectious eMLV production on the EL4 mouse lymphoma model.

A, Tumor growth following subcutaneous inoculation of EL4 or EL4.BU cells (both CD45.2⁺) into either CD45.1⁺ WT or CD45.1⁺ *Emv2*^{-/-} hosts. Plotted are the means (\pm SEM) of 8-19 mice/group. B, Subcutaneous tumor masses at the end of the observation period (day 11) in the groups described in A. Bar: 0.5 cm. C, Subcutaneous tumor weights in the same mice as in A and B. D, Frequency of host hematopoietic cells (CD45.1⁺) infiltrating the tumors in the same groups described in A. In C and D, each symbol is an individual mouse. E, Cellular composition of immune infiltrates isolated from tumor masses

described in A. Shown are the means of 4-5 mice/group. F, Expression of *Gzmb*, *Ifng*, *Il10*, and *Prfl* RNA in CD8⁺ T cells and *Gzmb*, *Ifng*, *Il10*, and *Il4* RNA in CD4⁺ T cells, purified from the indicated combination of tumor cell and host. Data are the mean expression of each gene normalized against *Hprt* expression in T cells from 4-5 mice/group. Numbers in A denote the *p* value from two-way ANOVA comparisons and in C and D from one-way ANOVA on ranks.

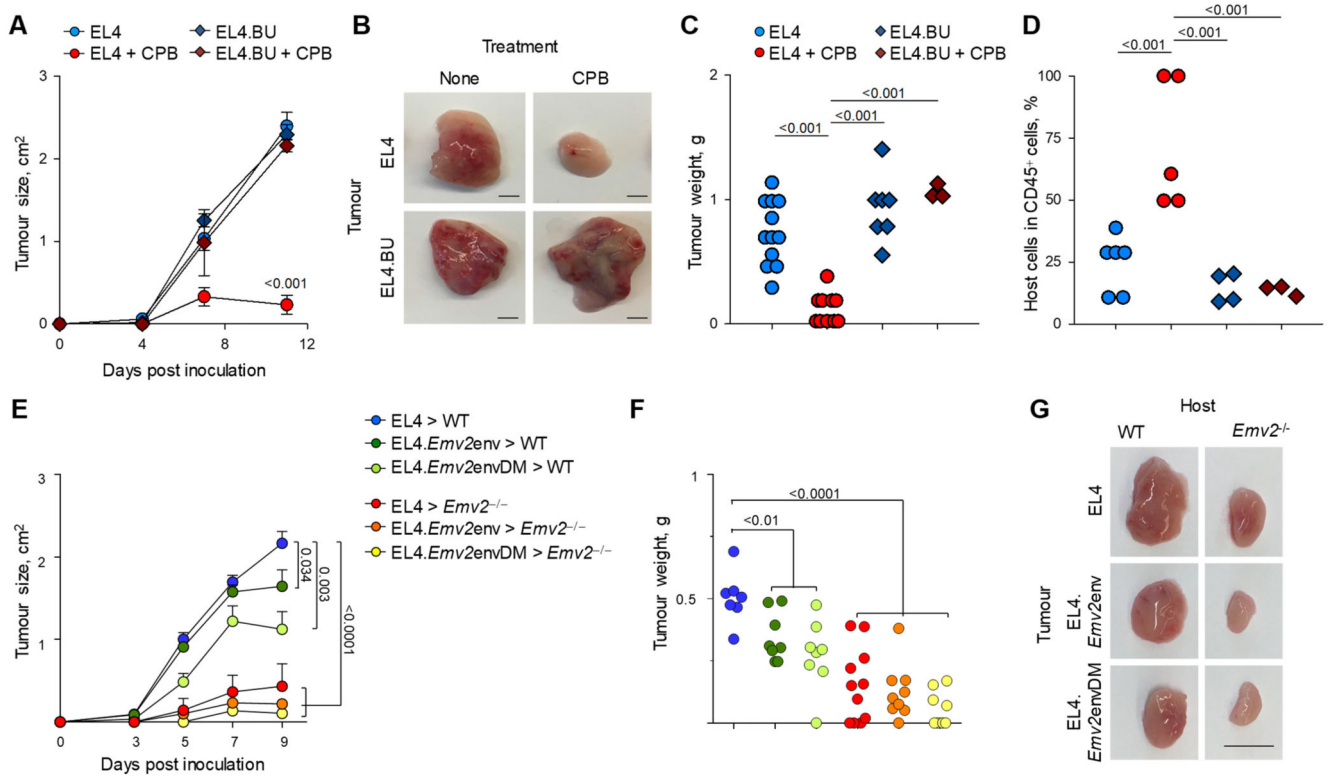


Figure 4. Impact of infectious eMLV production on EL4 response to immunotherapy and contribution of envelope-mediated immunosuppression.

A, Tumor growth following subcutaneous inoculation of 2×10^6 EL4 or EL4.BU cells into WT hosts with or without administration of anti-CTLA-4 and anti-PD-L1 therapy. Plotted are the means (\pm SEM) of 6-12 mice/group. 3/6 mice in the immunotherapy-treated EL4.BU group did not reach the end of the observation period due to the size of their tumors. B, Subcutaneous tumor masses at the end of the observation period (day 11) in the groups described in A. C, Subcutaneous tumor weights in the same mice as in A and B. D, Frequency of host hematopoietic cells infiltrating the tumors in the same groups described in A. E, Tumor growth following subcutaneous inoculation of 2×10^6 parental EL4 cells or EL4 cells overexpressing the WT *Emv2* envelope glycoprotein (EL4.*Emv2env*) or an ISD mutant (EL4.*Emv2envDM*), inoculated either in WT or *Emv2*^{-/-} hosts. Plotted are the means (\pm SEM) of 7-11 mice/group. F, Subcutaneous tumor weights in the same mice as in E. G, Subcutaneous tumor masses at the end of the observation period (day 9) in the groups described in F. In B and G, the bar denotes 0.5 cm. In C, D and F, each symbol is an individual mouse. Numbers in A and E denote the *p* value from two-way ANOVA comparisons and in C, D and F from one-way ANOVA on ranks.